

## One Water Molecule Stabilizes the Cationized Arginine Zwitterion

Matthew F. Bush, James S. Prell, Richard J. Saykally, and Evan R. Williams\*

*Contribution from the Department of Chemistry, University of California, Berkeley, California 94720-1460*

Received May 25, 2007; E-mail: williams@cchem.berkeley.edu

**Abstract:** Singly hydrated clusters of lithiated arginine, sodiated arginine, and lithiated arginine methyl ester are investigated using infrared action spectroscopy and computational chemistry. Whereas unsolvated lithiated arginine is nonzwitterionic, these results provide compelling evidence that attachment of a single water molecule to this ion makes the zwitterionic form of arginine, in which the side chain is protonated, more stable. The experimental spectra of lithiated and sodiated arginine with one water molecule are very similar and contain spectral signatures for protonated side chains, whereas those of lithiated arginine and singly hydrated lithiated arginine methyl ester are different and contain spectral signatures for neutral side chains. Calculations at the B3LYP/6-31++G\*\* level of theory indicate that solvating lithiated arginine with a single water molecule preferentially stabilizes the zwitterionic forms of this ion by 25–32 kJ/mol and two essentially isoenergetic zwitterionic structure are most stable. In these structures, the metal ion either coordinates with the N-terminal amino group and an oxygen atom of the carboxylate group (NO coordinated) or with both oxygen atoms of the carboxylate group (OO coordinated). In contrast, the OO-coordinated zwitterionic structure of sodiated arginine, both with and without a water molecule, is clearly lowest in energy for both ions. Hydration of the metal ion in these clusters weakens the interactions between the metal ion and the amino acid, whereas hydrogen-bond strengths are largely unaffected. Thus, hydration preferentially stabilizes the zwitterionic structures, all of which contain strong hydrogen bonds. Metal ion size strongly affects the relative propensity for these ions to form NO or OO coordinated structures and results in different zwitterionic structures for lithiated and sodiated arginine clusters containing one water molecule.

### Introduction

Neighboring molecules and ions can affect the stability of amino acid zwitterions. The zwitterionic form of isolated glycine is not a local minimum structure,<sup>1</sup> and calculations suggest that this form is ~90 kJ/mol higher in energy than the lowest-energy nonzwitterionic form.<sup>2</sup> Calculations also indicate that a single water molecule can make the zwitterionic structure a local minimum,<sup>3,4</sup> although this structure is still ~60 kJ/mol higher in energy than the lowest-energy nonzwitterionic structure. Additional water molecules preferentially stabilize the zwitterionic forms of glycine, and those forms are calculated to be lowest in energy when solvated by at least seven water molecules at the MP2/HF/6-31++G\*\* level of theory.<sup>4</sup> Additional computational studies have indicated similar minimum cluster sizes for zwitterion formation of microsolvated glycine clusters.<sup>2,5–7</sup>

It is extremely challenging to obtain compelling experimental evidence for the conversion from a nonzwitterionic form of an amino acid to the zwitterionic form with increasing hydrated cluster size. Pioneering spectroscopic experiments by Peteanu and Levy on tryptophan–water clusters generated in a free jet expansion show that the amine group of the side chain is the preferred site of water binding.<sup>8</sup> Doubly resonant two-photon ionization (R2PI), UV hole burning, IR-dip, and mass spectrometry experiments by Simons and co-workers show no compelling evidence for zwitterionic forms of tryptophan (Trp) when solvated by up to three water molecules.<sup>9–11</sup> Recently reported IR-dip spectra by Oomens and co-workers for Trp(H<sub>2</sub>O)<sub>1–6</sub> and Trp(MeOH)<sub>1–9</sub> exhibit spectral signatures for protonated amine and carboxylate functional groups with increasing cluster size and provide compelling evidence for a gradual transition to the zwitterionic form of tryptophan with increasing solvation.<sup>12</sup> Bowen and co-workers reported an onset

- (1) Ding, Y. B.; Krogh-Jespersen, K. *Chem. Phys. Lett.* **1992**, *199*, 261–266.
- (2) Kassab, E.; Langlet, J.; Evleth, E.; Akacem, Y. *J. Mol. Struct. (THEOCHEM)* **2000**, *531*, 267–282.
- (3) Ding, Y. B.; Krogh-Jespersen, K. *J. Comput. Chem.* **1996**, *17*, 338–349.
- (4) Aikens, C. M.; Gordon, M. S. *J. Am. Chem. Soc.* **2006**, *128*, 12835–12850.
- (5) Rzepa, H. S.; Man, Y. Y. *J. Chem. Soc., Perkin Trans. 2* **1991**, 531–537.
- (6) Balta, B.; Aviyente, V. *J. Comput. Chem.* **2003**, *24*, 1789–1802.
- (7) Fernandez-Ramos, A.; Smedarchina, Z.; Siebrand, W.; Zgierski, M. Z. *J. Chem. Phys.* **2000**, *113*, 9714–9721.

- (8) Peteanu, L. A.; Levy, D. H. *J. Phys. Chem.* **1988**, *92*, 6554–6561.
- (9) Snoek, L. C.; Kroemer, R. T.; Hockridge, M. R.; Simons, J. P. *Phys. Chem. Chem. Phys.* **2001**, *3*, 1819–1826.
- (10) Snoek, L. C.; Kroemer, R. T.; Simons, J. P. *Phys. Chem. Chem. Phys.* **2002**, *4*, 2130–2139.
- (11) Çarçabal, P.; Kroemer, R. T.; Snoek, L. C.; Simons, J. P.; Bakker, J. M.; Compagnon, I.; Meijer, G.; von Helden, G. *Phys. Chem. Chem. Phys.* **2004**, *6*, 4546–4552.
- (12) Blom, M. N.; Compagnon, I.; Polfer, N. C.; von Helden, G.; Meijer, G.; Suhai, S.; Paizs, B.; Oomens, J. *J. Phys. Chem. A* **2007**, *111*, 7309–7316.

for the formation of  $\text{Gly}\cdot\text{e}^-(\text{H}_2\text{O})_n$  at  $n = 5$  and suggested that a minimum of five water molecules are needed to form zwitterionic glycine in the neutral hydrated cluster.<sup>13</sup> However, Johnson and co-workers generated clusters for smaller  $n$  and suggested that the previously observed minimum cluster size<sup>13</sup> was due to source conditions rather than an indication of the onset of zwitterion formation.<sup>14,15</sup>

A number of studies have addressed the effects of water on the structures of cationized amino acids. Calculations indicate that solvating lithiated glutamine<sup>16</sup> and lysine<sup>17</sup> with one water molecule preferentially stabilizes the zwitterionic forms of these amino acids by 17 and 23 kJ/mol, respectively, although the nonzwitterionic forms of these singly hydrated, lithiated amino acids are lowest in energy and are the forms observed experimentally.<sup>16,17</sup> Additional calculations indicate that the zwitterionic forms of lithiated and sodiated glutamine solvated by two water molecules are lowest in energy, although blackbody infrared radiative dissociation (BIRD) experiments indicate that both complexes are nonzwitterionic.<sup>18</sup> Interestingly, similar calculations indicate that solvating sodiated proline,<sup>19,20</sup>  $\alpha$ -methyl-proline,<sup>21</sup> and valine<sup>22</sup> with one water molecule preferentially stabilizes the *nonzwitterionic* forms of these amino acids by 3–8 kJ/mol. BIRD experiments,<sup>23–25</sup> infrared (IR) action spectroscopy,<sup>26</sup> and MP2 calculations<sup>25</sup> indicate that lithiated valine with one and two water molecules are nonzwitterionic, with the metal ion coordinated to the N-terminal amino group and the carbonyl oxygen. With three water molecules, the metal ion interacts with both oxygen atoms of valine,<sup>24–26</sup> although the IR action spectrum of this ion shows no evidence for zwitterion formation.<sup>26</sup>

The proton affinity of the proton-accepting group can contribute to gas-phase zwitterion stability.<sup>22,27–31</sup> Although the proton affinity of arginine (Arg) is the highest of the naturally occurring amino acids<sup>32</sup> and the zwitterionic and nonzwitterionic

forms of Arg are close in energy,<sup>33</sup> IR cavity ringdown spectroscopy<sup>34</sup> and high-level ab initio calculations<sup>35–37</sup> both indicate that the nonzwitterionic form of isolated arginine is lowest in energy. The structures of cationized arginine have been of intense recent interest. Calculations,<sup>38,39</sup> dissociation experiments,<sup>39–41</sup> and IR multiple photon dissociation (IRMPD) spectra<sup>38</sup> indicate that  $\text{Arg}\cdot\text{Li}^+$  is nonzwitterionic and that the zwitterionic form of arginine, in which the side chain is protonated, is preferentially stabilized with increasing alkali metal ion size. Deconvolution of the IRMPD spectrum of  $\text{Arg}\cdot\text{Na}^+$  suggests that roughly 90% of the ions are zwitterionic and that of  $\text{Arg}\cdot\text{K}^+$  shows no evidence for the nonzwitterionic structure.<sup>38</sup> Calculations indicate that the lowest-energy form of  $\text{Arg}\cdot\text{Ag}^+$  is nonzwitterionic.<sup>42</sup>

IRMPD action spectroscopy, using light from either free electron lasers (typically 5–10  $\mu\text{m}$ ) or benchtop laser systems based on optical parametric generation (typically 2.5–4  $\mu\text{m}$ ), has emerged as a powerful method to probe the structures of protonated and metal cationized amino acid clusters in the gas phase. In pioneering experiments by McLafferty and co-workers, IRMPD spectra in the hydrogen-stretch region indicate that the protonated homodimer of glycine is nonzwitterionic, whereas the protonated heterodimer consisting of glycine and lysine is zwitterionic.<sup>43</sup> IRMPD spectra in the fingerprint region by Wu and McMahon confirmed that the protonated homodimer of glycine is nonzwitterionic and revealed that the protonated homodimer of proline has both nonzwitterionic and zwitterionic populations under the conditions of their experiments.<sup>44</sup> The relative intensity of the free carboxylic acid OH stretch in  $\text{serine}_n\cdot\text{H}^+$ ,  $n = 2–8$ , decreases with increasing cluster size, indicating that this band is depleted through the formation of zwitterionic structures or that the carboxylic acid OH stretch is red-shifted due to hydrogen bond formation.<sup>45</sup> IRMPD spectra of sodiated glycine and proline provide spectral signatures for both the nonzwitterionic and zwitterionic forms of cationized aliphatic amino acids in the 5–10  $\mu\text{m}$  region.<sup>46</sup> Subsequent studies in this frequency range have revealed the nature of metal ion binding in cationized clusters of aromatic amino acids,<sup>47–49</sup> the formation of amino acid zwitterions during gas-phase H/D

- (13) Xu, S.; Nilles, J. M.; Bowen, K. H. *J. Chem. Phys.* **2003**, *119*, 10696–10701.
- (14) Diken, E. G.; Hammer, N. I.; Johnson, M. A. *J. Chem. Phys.* **2004**, *120*, 9899–9902.
- (15) Diken, E. G.; Headrick, J. M.; Johnson, M. A. *J. Chem. Phys.* **2005**, *122*, 224317.
- (16) Lemoff, A. S.; Bush, M. F.; Wu, C. C.; Williams, E. R. *J. Am. Chem. Soc.* **2005**, *127*, 10276–10286.
- (17) Lemoff, A. S.; Bush, M. F.; O'Brien, J. T.; Williams, E. R. *J. Phys. Chem. A* **2006**, *110*, 8433–8442.
- (18) Lemoff, A. S.; Wu, C. C.; Bush, M. F.; Williams, E. R. *J. Phys. Chem. A* **2006**, *110*, 3662–3669.
- (19) Moision, R. M.; Armentrout, P. B. *J. Phys. Chem. A* **2006**, *110*, 3933–3946.
- (20) Ye, S. J.; Moision, R. M.; Armentrout, P. B. *Int. J. Mass Spectrom.* **2006**, *253*, 288–304.
- (21) Lemoff, A. S.; Bush, M. F.; Williams, E. R. *J. Phys. Chem. A* **2005**, *109*, 1903–1910.
- (22) Lemoff, A. S.; Bush, M. F.; Williams, E. R. *J. Am. Chem. Soc.* **2003**, *125*, 13576–13584.
- (23) Jockusch, R. A.; Lemoff, A. S.; Williams, E. R. *J. Am. Chem. Soc.* **2001**, *123*, 12255–12265.
- (24) Lemoff, A. S.; Williams, E. R. *J. Am. Chem. Soc.* **2004**, *126*, 1014–1024.
- (25) Jockusch, R. A.; Rizzo, T. R.; Williams, E. R. *J. Phys. Chem. A* **2001**, *105*, 10929–10942.
- (26) Kamariotis, A.; Boyarkin, O. V.; Mercier, S. R.; Beck, R. D.; Bush, M. F.; Williams, E. R.; Rizzo, T. R. *J. Am. Chem. Soc.* **2006**, *128*, 905–916.
- (27) Strittmatter, E. F.; Williams, E. R. *Int. J. Mass Spectrom.* **2001**, *212*, 287–300.
- (28) Strittmatter, E. F.; Wong, R. L.; Williams, E. R. *J. Phys. Chem. A* **2000**, *104*, 10271–10279.
- (29) Wyttenbach, T.; Witt, M.; Bowers, M. T. *J. Am. Chem. Soc.* **2000**, *122*, 3458–3464.
- (30) Julian, R. R.; Jarrold, M. F. *J. Phys. Chem. A* **2004**, *108*, 10861–10864.
- (31) Bush, M. F.; Forbes, M. G.; Jockusch, R. A.; Oomens, J.; Polfer, N. C.; Saykally, R. J.; Williams, E. R. *J. Phys. Chem. A* **2007**, *111*, 7753–7760.
- (32) Bleiholder, C.; Suhai, S.; Paizs, B. *J. Am. Soc. Mass Spectrom.* **2006**, *17*, 1275–1281.

- (33) Price, W. D.; Jockusch, R. A.; Williams, E. R. *J. Am. Chem. Soc.* **1997**, *119*, 11988–11989.
- (34) Chapo, C. J.; Paul, J. B.; Provencal, R. A.; Roth, K.; Saykally, R. J. *J. Am. Chem. Soc.* **1998**, *120*, 12956–12957.
- (35) Ling, S. L.; Yu, W. B.; Huang, Z. J.; Lin, Z. J.; Haranczyk, M.; Gutowski, M. *J. Phys. Chem. A* **2006**, *110*, 12282–12291.
- (36) Julian, R. R.; Beauchamp, J. L.; Goddard, W. A. *J. Phys. Chem. A* **2002**, *106*, 32–34.
- (37) Rak, J.; Skurski, P.; Simons, J.; Gutowski, M. *J. Am. Chem. Soc.* **2001**, *123*, 11695–11707.
- (38) Bush, M. F.; O'Brien, J. T.; Prell, J. S.; Saykally, R. J.; Williams, E. R. *J. Am. Chem. Soc.* **2007**, *129*, 1612–1622.
- (39) Jockusch, R. A.; Price, W. D.; Williams, E. R. *J. Phys. Chem. A* **1999**, *103*, 9266–9274.
- (40) Cerda, B. A.; Wesdemiotis, C. *Analyst* **2000**, *125*, 657–660.
- (41) Talley, J. M.; Cerda, B. A.; Ohanessian, G.; Wesdemiotis, C. *Chem.—Eur. J.* **2002**, *8*, 1377–1388.
- (42) Shoeib, T.; Siu, K. W. M.; Hopkinson, A. C. *J. Phys. Chem. A* **2002**, *106*, 6121–6128.
- (43) Oh, H. B.; Lin, C.; Hwang, H. Y.; Zhai, H. L.; Breuker, K.; Zabravskov, V.; Carpenter, B. K.; McLafferty, F. W. *J. Am. Chem. Soc.* **2005**, *127*, 4076–4083.
- (44) Wu, R.; McMahon, T. B. *J. Am. Chem. Soc.* **2007**, *129*, 4864–4865.
- (45) Kong, X. L.; Tsai, I. A.; Sabu, S.; Han, C. C.; Lee, Y. T.; Chang, H. C.; Tu, S. Y.; Kung, A. H.; Wu, C. C. *Angew. Chem., Int. Ed.* **2006**, *45*, 4130–4134.
- (46) Kapota, C.; Lemaire, J.; Maître, P.; Ohanessian, G. *J. Am. Chem. Soc.* **2004**, *126*, 1836–1842.
- (47) Polfer, N. C.; Oomens, J.; Dunbar, R. C. *Phys. Chem. Chem. Phys.* **2006**, *8*, 2744–2751.
- (48) Polfer, N. C.; Oomens, J.; Moore, D. T.; von Helden, G.; Meijer, G.; Dunbar, R. C. *J. Am. Chem. Soc.* **2006**, *128*, 517–525.

exchange,<sup>50</sup> and zwitterion formation with increasing metal ion size in basic amino acids.<sup>31</sup> Elegant experiments by Rizzo and co-workers have demonstrated the use of these techniques to study hydrated amino acids in the gas phase.<sup>26</sup>

Here, IRMPD spectra in the hydrogen-stretch region and complementary ab initio calculations indicate that one water molecule preferentially stabilizes the zwitterionic forms of these amino acids and significantly affects the structure of lithiated arginine. This is the first direct spectroscopic probe indicating that hydration by an explicit number of water molecules can induce the transformation from nonzwitterionic to zwitterionic structure for an amino acid.

## Methods

Experiments were performed on a 2.7 T Fourier-transform ion cyclotron resonance mass spectrometer. The instrument and general experimental methods are described elsewhere.<sup>38</sup>  $\text{Arg}\bullet\text{M}^+(\text{H}_2\text{O})$ ,  $\text{M} = \text{Li}$  and  $\text{Na}$ , clusters are formed by nanoelectrospray ionization from aqueous solutions of 500  $\mu\text{M}$   $\text{Arg}\bullet\text{HCl}$  and 2 mM MOH using a home-built electrospray interface.<sup>51</sup> For  $\text{ArgOMe}\bullet\text{Li}^+(\text{H}_2\text{O})$ , solutions of 500  $\mu\text{M}$   $\text{ArgOMe}\bullet 2\text{HCl}$  and 2 mM LiOH were prepared in methanol, and hydrated ions were formed by condensation of atmospheric water vapor in the electrospray interface.<sup>52</sup>  $\text{ArgOMe}$  rapidly degraded in aqueous solutions that yielded metal cationized clusters.  $\text{Arg}\bullet\text{HCl}$ ,  $\text{ArgOMe}\bullet 2\text{HCl}$ , LiOH, NaOH, and methanol were purchased from Sigma Chemical Co. (St. Louis, MO), Alfa Aesar (Ward Hill, MA), Aldrich Chemical Co. (Milwaukee, WI), Fischer Scientific (Pittsburgh, PA), and EMD Chemicals (Gibbstown, NJ), respectively, and were used without further purification. Ions were trapped in a cylindrical ion cell cooled to 200 or 240 K with a regulated flow of liquid nitrogen.<sup>53</sup> The cluster of interest was isolated using a stored waveform inverse Fourier transform and subsequently irradiated with 40–600 pulses of IR radiation (8–21 mJ per  $\sim 7$  ns pulse) from a tunable 10 Hz optical parametric oscillator/amplifier (LaserVision, Bellevue, WA). The loss of a water molecule is the only photodissociation product observed, and each IRMPD spectrum was obtained by plotting the power- and time-corrected photodissociation intensity as a function of laser frequency.<sup>38</sup> Blackbody infrared radiative dissociation experiments were performed using the methods discussed above. First-order rate constants were determined from the slope of  $\ln([\text{Arg}\bullet\text{M}^+(\text{H}_2\text{O})_n]/([\text{Arg}\bullet\text{M}^+(\text{H}_2\text{O})_n] + [\text{Arg}\bullet\text{M}^+(\text{H}_2\text{O})_{n-1}] + \dots))$  versus time. The data are fit well by straight lines with  $R^2$  correlation coefficients  $\geq 0.995$ .

The majority of calculations were performed using methods described in the previous investigation of  $\text{Arg}\bullet\text{M}^+$  and  $\text{ArgOMe}\bullet\text{M}^+$ .<sup>38</sup> Briefly, candidate structures were generated using Monte Carlo conformational searching with the MMFF94 force field and then energy minimized with hybrid method density functional theory (B3LYP) calculations with the 6-31++G\*\* basis set using MacroModel 8.1 and Jaguar 6.5 (Schrödinger, Inc., Portland, OR), respectively. Vibrational frequencies and intensities were calculated using the “double-harmonic” approximation (linear dipole moment function and harmonic potentials). For calculated vibrational spectra, frequencies were scaled by 0.95 and convolved using 20  $\text{cm}^{-1}$  fwhm Lorentzian distributions. For bands with unambiguous assignments, this scaling factor yielded good agreement between experiment and theory and was used previously to compare infrared action spectra and calculations at this level of theory

for cationized arginine.<sup>38</sup> Additional calculations used initial geometries obtained from the B3LYP/6-31++G\*\* calculations described above and were performed using Q-Chem v3.0 (Pittsburgh, PA).<sup>54</sup>

## Results and Discussion

Infrared action spectra were acquired by simultaneously measuring precursor and fragment ion intensities as a function of laser irradiation frequency. The internal energy distribution of the ions under the experimental conditions prior to laser irradiation should closely resemble a Boltzmann distribution.<sup>55</sup> In 30 s with a copper jacket temperature of 200 K, no blackbody infrared radiative dissociation (BIRD) was observed for  $\text{Arg}\bullet\text{Li}^+(\text{H}_2\text{O})$  and only 4% of the  $\text{Arg}\bullet\text{Na}^+(\text{H}_2\text{O})$  precursor ions dissociate. At the slightly higher copper jacket temperature of 240 K, 18 and 38% of the lithiated and sodiated precursor ions dissociate, respectively, suggesting that the absorption of a single laser photon may be adequate to induce photodissociation for a significant fraction of the ion population. A single photon infrared action spectrum should be very similar to the linear infrared absorption spectrum of the ion. When absorption does not yield photodissociation, the resulting ion will have increased internal energy and may relax via radiative emission<sup>55,56</sup> or photodissociate upon the absorption of an additional photon or photons. At lower frequencies, multiple photon processes are likely increasingly important due to reduced internal energy deposition, and the resulting band intensities may deviate from the linear absorption spectrum. Experimental spectra will therefore be referred to as infrared multiple photon dissociation (IRMPD) spectra to emphasize the potential differences between these action spectra and pure absorption spectra.

The IRMPD spectra of  $\text{Arg}\bullet\text{M}^+$ ,  $\text{M} = \text{Li}$  and  $\text{Na}$ , are different and indicate that Arg is nonzwitterionic in the former and predominately zwitterionic in the latter.<sup>38</sup> In contrast, the IRMPD spectra of  $\text{Arg}\bullet\text{M}^+(\text{H}_2\text{O})$ ,  $\text{M} = \text{Li}$  and  $\text{Na}$ , are similar in the hydrogen-stretch region, suggesting that both ions have related structures (Figure 1). The highest-frequency bands in these spectra occur near 3640 and 3720  $\text{cm}^{-1}$ . Bands at similar frequencies were also observed for valine $\bullet\text{Li}^+(\text{H}_2\text{O})$  and assigned to the symmetric and asymmetric stretches of the solvating water molecule, respectively.<sup>26</sup> The presence of both bands at high frequency indicates the presence of an acceptor-only water molecule; the symmetric stretch of a water molecule that donates a hydrogen bond is significantly red-shifted.<sup>26</sup> The weak bands close in frequency to the fundamental water stretches are probably combination and difference bands involving the fundamental stretching transitions and low-frequency transitions, such as the water out-of-plane bend. These bands provide only limited structural information and are not analyzed further here. The lower-frequency bands ( $< 3600 \text{ cm}^{-1}$ ) in the IRMPD spectra of  $\text{Arg}\bullet\text{M}^+(\text{H}_2\text{O})$  and  $\text{ArgOMe}\bullet\text{Li}^+(\text{H}_2\text{O})$  are therefore assigned to hydrogen stretches of Arg and ArgOMe, not those of the solvating water molecule.

Arginine methyl ester (ArgOMe) lacks the carboxylic acid group of Arg and cannot form zwitterionic structures. If the structures of  $\text{Arg}\bullet\text{M}^+(\text{H}_2\text{O})$ ,  $\text{M} = \text{Li}$  and  $\text{Na}$ , and  $\text{ArgOMe}\bullet\text{Li}^+(\text{H}_2\text{O})$  were similar, the IRMPD spectra of  $\text{Arg}\bullet\text{M}^+(\text{H}_2\text{O})$  would be expected to contain the bands observed for  $\text{ArgOMe}\bullet\text{Li}^+$

(49) Polfer, N. C.; Paizs, B.; Snoek, L. C.; Compagnon, I.; Suhai, S.; Meijer, G.; von Helden, G.; Oomens, J. *J. Am. Chem. Soc.* **2005**, *127*, 8571–8579.

(50) Polfer, N. C.; Dunbar, R. C.; Oomens, J. *J. Am. Soc. Mass Spectrom.* **2007**, *18*, 512–516.

(51) Bush, M. F.; Saykally, R. J.; Williams, E. R. *Int. J. Mass Spectrom.* **2006**, *253*, 256–262.

(52) Rodriguez-Cruz, S. E.; Klassen, J. S.; Williams, E. R. *J. Am. Soc. Mass Spectrom.* **1999**, *10*, 958–968.

(53) Wong, R. L.; Paech, K.; Williams, E. R. *Int. J. Mass Spectrom.* **2004**, *232*, 59–66.

(54) Shao, Y.; et al. *Phys. Chem. Chem. Phys.* **2006**, *8*, 3172–3191.

(55) Price, W. D.; Schnier, P. D.; Jockusch, R. A.; Strittmatter, E. F.; Williams, E. R. *J. Am. Chem. Soc.* **1996**, *118*, 10640–10644.

(56) Dunbar, R. C. *Mass Spectrom. Rev.* **1992**, *11*, 309–339.



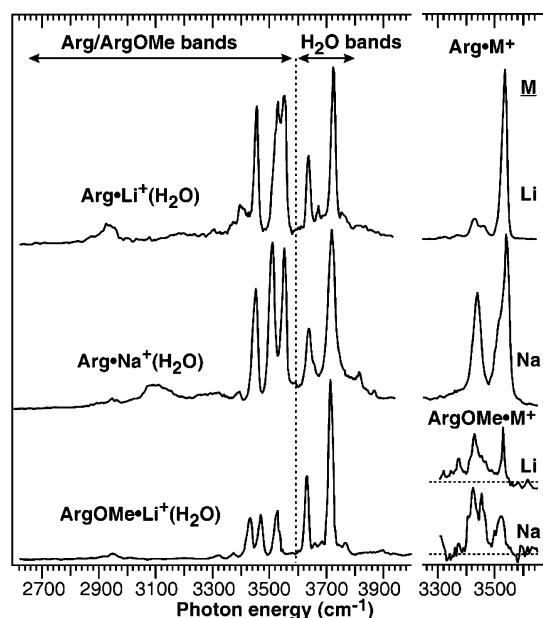


**Figure 1.** Photodissociation spectra of  $\text{Arg}\cdot\text{Li}^+(\text{H}_2\text{O})$ ,  $\text{Arg}\cdot\text{Na}^+(\text{H}_2\text{O})$ , and  $\text{ArgOMe}\cdot\text{Li}^+(\text{H}_2\text{O})$  obtained with a copper jacket temperature of 200 K (left). Selected regions of previously reported photodissociation spectra of  $\text{Arg}\cdot\text{M}^+$  and  $\text{ArgOMe}\cdot\text{M}^+$ ,  $\text{M} = \text{Li}$  and  $\text{Na}$ , are included for comparison (right).<sup>38</sup> The spectrum of  $\text{Arg}\cdot\text{Na}^+(\text{H}_2\text{O})$  was also acquired from 2000–2600  $\text{cm}^{-1}$ , but no photodissociation was observed.

( $\text{H}_2\text{O}$ ) and an additional strong band near 3540  $\text{cm}^{-1}$  corresponding to the free acid OH stretch.<sup>26,38</sup> This does not appear to be the case; therefore, the structure of  $\text{Arg}\cdot\text{M}^+(\text{H}_2\text{O})$  is unlikely to resemble that of  $\text{ArgOMe}\cdot\text{Li}^+(\text{H}_2\text{O})$ . Furthermore, the IRMPD spectrum of  $\text{Arg}\cdot\text{Li}^+(\text{H}_2\text{O})$  obtained below 3600  $\text{cm}^{-1}$  does not resemble that obtained previously for  $\text{Arg}\cdot\text{Li}^+$ .<sup>38</sup> These data indicate that the structures of  $\text{Arg}\cdot\text{Li}^+$  and  $\text{Arg}\cdot\text{M}^+(\text{H}_2\text{O})$  are different and that Arg in the latter is zwitterionic.

Although considerable structural information (zwitterion versus nonzwitterion, mode of water binding, etc.) is obtained from inspection of the IRMPD spectra and comparisons with spectra reported previously, additional insights can be gained through comparisons with spectra calculated for low-energy candidate structure using density functional theory. Only the lowest-energy structures identified and those that illustrate important bonding motifs are presented because the conformational spaces of these ions are extremely large. Results for some additional candidate structures are reported in the Supporting Information. In addition, there are the attendant uncertainties in comparing absorbance spectra calculated at zero K using the double-harmonic approximation with experimental action spectra obtained at finite temperatures.

**Low-Energy Structures.** The low-energy structural families of  $\text{Arg}\cdot\text{Li}^+(\text{H}_2\text{O})$  (Figure 2) are very similar to those found previously for  $\text{Arg}\cdot\text{Li}^+$ .<sup>38</sup> For clarity, the previously identified  $\text{Arg}\cdot\text{Li}^+$  structures are designated  $\mathbf{x0}$ ,  $\mathbf{x} = \mathbf{A}–\mathbf{J}$ , and the related  $\text{Arg}\cdot\text{Li}^+(\text{H}_2\text{O})$  structures are designated  $\mathbf{x1}$ . Relative free energies at 0, 200, and 298 K for all structures are reported in Table 1. For all structural families except **C1**, the water molecule directly solvates the metal ion in the corresponding  $\mathbf{x0}$  structure and no additional interactions are formed. For **C1**, the water molecule solvates the metal ion and accepts a weak hydrogen bond from the guanidino side chain.

Additional structures of  $\text{Arg}\cdot\text{Li}^+(\text{H}_2\text{O})$ , in which the water molecule displaces the metal ion, are designated  $\mathbf{x1}^*$  and were

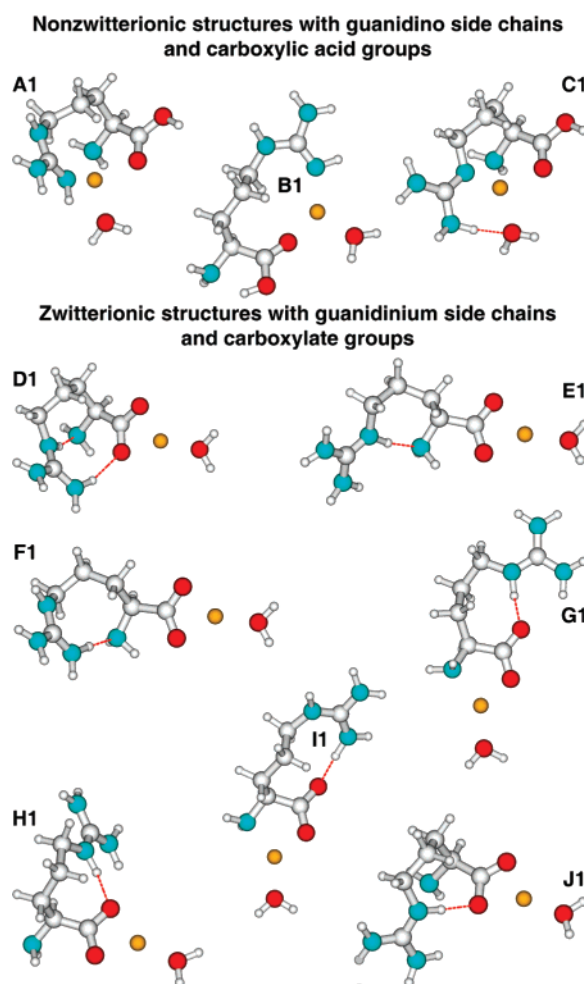


**Figure 2.** Energy minimized structures **A1**–**J1** of the nonzwitterionic and zwitterionic forms of  $\text{Arg}\cdot\text{Li}^+(\text{H}_2\text{O})$  from B3LYP/6-31++G\*\* calculations.

**Table 1.** Relative Zero-Point Corrected Free Energies<sup>a</sup> at 0, 200, and 298 K of  $\text{Arg}\cdot\text{Li}^+(\text{H}_2\text{O})$  and  $\text{Arg}\cdot\text{Na}^+(\text{H}_2\text{O})$  from B3LYP/6-31++G\*\* Calculations

	$\text{Arg}\cdot\text{Li}^+(\text{H}_2\text{O})$				$\text{Arg}\cdot\text{Na}^+(\text{H}_2\text{O})$		
	$\Delta H_{0\text{K}}$	$\Delta G_{200\text{K}}$	$\Delta G_{298\text{K}}$		$\Delta H_{0\text{K}}$	$\Delta G_{200\text{K}}$	$\Delta G_{298\text{K}}$
<b>A1/A1*</b>	16/33	18/36	20/39	<b>A1</b>	22	19	18
<b>B1</b>	18	20	21	<b>B1</b>	36	31	29
<b>C1</b>	28	31	34	<b>C1</b>	43	41	42
<b>D1/D1*</b>	0/7	0/11	0.03/14	<b>D1/D1*</b>	2/0	0.3/0	0/2
<b>E1/E1*</b>	11/16	10/17	8/18	<b>E1/E1*</b>	22/12	17/9	15/8
<b>F1/F1*</b>	15/20	14/23	13/26	<b>F1</b>	15	10	7
<b>G1/G1*</b>	1/21	0.5/23	0/25	<b>G1/G1*</b>	15/15	13/13	11/12
<b>H1</b>	18	16	14	<b>H1</b>	28	26	26
<b>I1</b>	9	12	14	<b>I1</b>	26	24	37
<b>J1/J1*</b>	20/26	18/28	17/28	<b>J1</b>	19	16	17

<sup>a</sup> All energies are in kJ/mol.

found to be at least 5 kJ/mol higher in energy than the corresponding  $\mathbf{x1}$  structure. In these structures, the water molecule solvates the metal ion and donates a hydrogen bond to the displaced ligand in the corresponding  $\mathbf{x0}$  structure. Analogous local minima have also been identified for numerous other hydrated amino acids.<sup>19–25</sup> For  $\text{Arg}\cdot\text{Na}^+(\text{H}_2\text{O})$ , some  $\mathbf{x1}^*$  structures were slightly lower in energy than the corresponding  $\mathbf{x1}$  structure. Additional  $\mathbf{x1}^*$  structures were identified in the conformational search and evaluated at the B3LYP/6-31G\* level of theory. However, the experimental spectra all contain a high-frequency water symmetric stretching band, a spectral signature

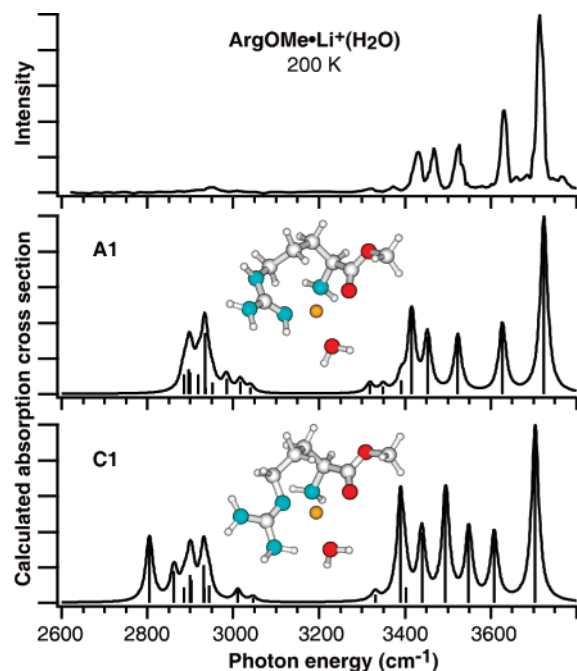


**Figure 3.** Photodissociation spectrum of  $\text{ArgOMe}\cdot\text{Li}^+(\text{H}_2\text{O})$  and B3LYP/6-31++G\*\* calculated spectra for both conformers of this ion.

for  $\mathbf{x1}$  structures, and additional calculations were performed only on selected  $\mathbf{x1}^*$  structures of greatest interest.

**Structure of  $\text{ArgOMe}\cdot\text{Li}^+(\text{H}_2\text{O})$ .** The lowest-energy structure of  $\text{ArgOMe}\cdot\text{Li}^+(\text{H}_2\text{O})$  is **A1**, in which the water molecule directly solvates the metal ion in the lowest-energy structure of  $\text{ArgOMe}\cdot\text{Li}^+$  (**A0**). Structure **C1** is 10, 13, and 12 kJ/mol higher in free energy than structure **A1** at 0, 200, and 298 K, respectively. These relative free energies are essentially identical to those for  $\text{Arg}\cdot\text{Li}^+(\text{H}_2\text{O})$ , indicating that lithiated arginine methyl ester is a very good structural analogue for structures **A1** and **C1** of lithiated arginine.

The IRMPD spectrum of  $\text{ArgOMe}\cdot\text{Li}^+(\text{H}_2\text{O})$  strongly resembles those obtained previously for  $\text{ArgOMe}\cdot\text{Li}^+$  and  $\text{ArgOMe}\cdot\text{Na}^+$ , which were assigned to structure **A0**,<sup>38</sup> superimposed on the stretching modes of the solvating water molecule (Figure 1). Furthermore, the IRMPD spectrum of  $\text{ArgOMe}\cdot\text{Li}^+(\text{H}_2\text{O})$  strongly resembles the calculated absorbance spectrum of structure **A1** (Figure 3). The experimental bands at 3320, 3370, 3430, 3470, 3525, 3630, and 3720  $\text{cm}^{-1}$  are close in both frequency and relative intensity to the calculated bands for the  $\text{N}_\eta\text{H}$  stretch (3349  $\text{cm}^{-1}$ ),  $\text{N}_\text{T}\text{H}_2$  asymmetric stretch (3391  $\text{cm}^{-1}$ ),  $\text{N}_\eta\text{H}_2$  symmetric stretch (3415  $\text{cm}^{-1}$ ),  $\text{N}_\epsilon\text{H}$  stretch (3452  $\text{cm}^{-1}$ ),  $\text{N}_\eta\text{H}_2$  asymmetric stretch (3523  $\text{cm}^{-1}$ ), water symmetric stretch (3627  $\text{cm}^{-1}$ ), and water asymmetric stretch (3724  $\text{cm}^{-1}$ ). The experimental spectrum also contains a band at 2940  $\text{cm}^{-1}$  which is assigned to the CH stretching modes of the cluster. These stretches are similar in frequency and oscillator strength for all calculated structures and thus provide only limited structural information. The experimental band height is notably less intense relative to those of the other bands in the spectrum than expected from the calculation, suggesting an error in the calculated intensities and/or reduced photodissociation efficiency for these modes, attributable to lower photon energies, lower laser power in this frequency range, or other factors.

The calculated absorbance spectrum for structure **C1** is a poorer match to the experimental spectrum. Notably, the

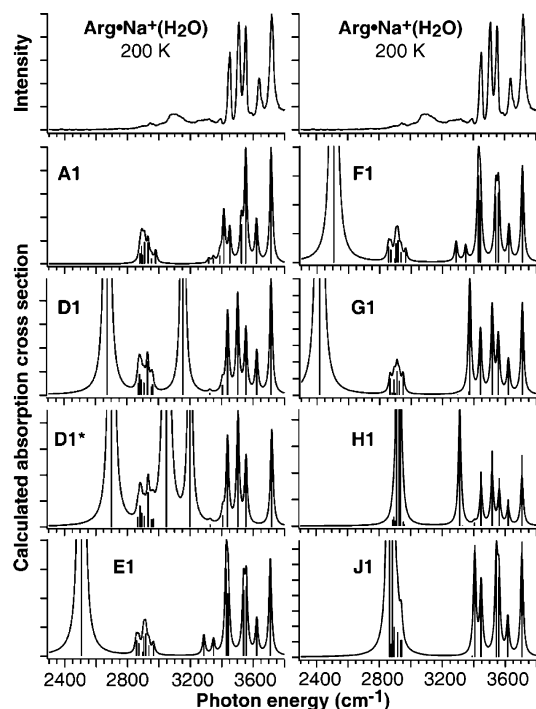


**Figure 4.** Photodissociation spectrum of  $\text{Arg}\cdot\text{Na}^+(\text{H}_2\text{O})$  and B3LYP/6-31++G\*\* calculated spectra for selected conformers of this ion. The intensities of the calculated spectra are scaled to the higher-frequency bands in the spectra. Un-normalized spectra and additional calculated spectra are shown in Supporting Information Figures 1–4.

calculated spectrum contains four intense bands associated with the guanidino side chain, whereas the experimental spectrum exhibits three such bands. Note that the water molecule in **C1** accepts a weak hydrogen bond from one of the  $\text{N}_\eta\text{H}_2$  groups, which was present in all energy-minimized structures of this family. The infrared absorbance spectrum for this structure without that hydrogen bond should be well approximated by a superposition of the fundamental water stretches and the spectrum calculated for **C0** of  $\text{ArgOMe}\cdot\text{Li}^+$ .<sup>38</sup> If that were the case, the spectrum would be expected to contain free  $\text{N}_\eta\text{H}_2$  asymmetric stretches at 3510 and 3560  $\text{cm}^{-1}$ , whereas the IRMPD spectrum contains only one band at 3525  $\text{cm}^{-1}$ .

The IRMPD spectrum of  $\text{ArgOMe}\cdot\text{Li}^+$  contains well-resolved bands at 3430 and 3530  $\text{cm}^{-1}$  bands, calculated for structure **A0**, but that at 3460  $\text{cm}^{-1}$  is not readily apparent (Figure 1).<sup>38</sup> The similarities between the bands common to the spectra for  $\text{ArgOMe}\cdot\text{Li}^+$ ,  $\text{ArgOMe}\cdot\text{Na}^+$ , and  $\text{ArgOMe}\cdot\text{Li}^+(\text{H}_2\text{O})$  suggest that arginine methyl ester adopts similar structures in all three clusters and that the band “missing” for  $\text{ArgOMe}\cdot\text{Li}^+$  is the result of poor signal-to-noise or other experimental factors, rather than a difference in structure.

**Structure of  $\text{Arg}\cdot\text{Na}^+(\text{H}_2\text{O})$ .** The IRMPD spectrum of  $\text{Arg}\cdot\text{Na}^+(\text{H}_2\text{O})$  has many resolved bands, although these bands are broader than those observed for  $\text{Arg}\cdot\text{Li}^+(\text{H}_2\text{O})$  which suggests that multiple conformers may contribute to the IRMPD spectrum (Figure 1). This spectrum does not resemble those of either structure (**A1** and **E1**, Figure 4) found to contribute to the IRMPD spectrum of the corresponding ion without a water molecule,<sup>38</sup> but rather resembles zwitterionic structures with multiple hydrogen-bonding interactions between the side chain and the amino acid backbone. Structure **A1** can be discounted on the basis of arguments analogous to those made for  $\text{Arg}\cdot\text{Li}^+$

**Table 2.** Frequencies (freq, cm<sup>-1</sup>) and Integrated Oscillator Intensities (int, km/mol) for Selected Bands of Arg•Li<sup>+</sup>(H<sub>2</sub>O) and Arg•Na<sup>+</sup>(H<sub>2</sub>O)

band	IRMPD freq	Arg•Li <sup>+</sup> (H <sub>2</sub> O)						IRMPD Freq	Arg•Na <sup>+</sup> (H <sub>2</sub> O)					
		D1		D1*		G1			D1		D1*		G1	
		freq	int	freq	int	freq	int		freq	int	freq	int	freq	int
N <sub>ε</sub> H stretch	-	2708	1340	2712	1348	2545	2198	—	2665	1364	2700	1354	2416	2365
N <sub>γ</sub> H <sub>2</sub> symmetric stretch	3400	3213	538	3247	430	3390	176	3200	3155	658	3198	504	3373	160
N <sub>γ</sub> H <sub>2</sub> symmetric stretch	3450	3438	97	3435	97	3440	96	3450	3438	93	3437	96	3441	92
N <sub>γ</sub> H <sub>2</sub> asymmetric stretch	3530	3508	124	3506	139	3539	130	3510	3502	113	3504	123	3516	124
N <sub>γ</sub> H <sub>2</sub> asymmetric stretch	3550	3558	79	3552	78	3558	90	3550	3554	73	3555	74	3555	80
H <sub>2</sub> O symmetric stretch	3640	3618	71	3039	1272	3620	69	3640	3623	49	3049	1456	3619	49
H <sub>2</sub> O asymmetric stretch	3720	3709	149	3723	140	3720	148	3720	3714	133	3719	108	3708	131

**Table 3.** Relative Energies<sup>a</sup> in kJ/mol of Structures **A1**, **D1**, **D1\***, and **G1** of Arg•Li<sup>+</sup>(H<sub>2</sub>O) at Various Levels of Theory

energy	geometry	structure			
		A1	D1	D1*	G1
B3LYP/6-31G**	B3LYP/6-31G**	15	0	10	5
B3LYP/6-31+G**	B3LYP/6-31+G**	16	0	9	6
B3LYP/6-31++G**	B3LYP/6-31++G**	17	0	8	2
B3LYP/6-311++G(2d,2p)	B3LYP/6-311++G**	13	0	7	1
B3LYP/cc-pVDZ	B3LYP/cc-pVDZ	7	0	7	1
B3LYP/cc-pVTZ	B3LYP/cc-pVDZ	13	1	8	0
RIMP2/cc-pVDZ	B3LYP/6-31++G**	0	10	23	20
RIMP2/cc-pVDZ	RIMP2/cc-pVDZ	0	10	23	20
MP2/cc-pVDZ	RIMP2/cc-pVDZ	0	10	23	20
RIMP2/cc-pVTZ	RIMP2/cc-pVDZ	0	1	10	10
MP2/6-311++G(2d,2p)	B3LYP/6-31++G**	5	0	2	20

<sup>a</sup> Electronic energies are from structures energy minimized using Q-Chem v3.0.<sup>54</sup> and include B3LYP/6-31++G\*\* zero-point energies calculated using Jaguar v6.5.

(H<sub>2</sub>O) (vide supra). The calculated spectrum of structure **E1** contains two N<sub>γ</sub>H<sub>2</sub> symmetric stretch bands at high frequencies, but the experimental spectrum contains only one band of significant intensity in this region (Table 2). The weak band near 3390 cm<sup>-1</sup> is likely due to the N<sub>γ</sub>H<sub>2</sub> asymmetric stretch, which is common to all of these structures, rather than to a small population of the **E1** conformer.

The IRMPD spectrum of Arg•Na<sup>+</sup>(H<sub>2</sub>O) is in good agreement with the calculated spectra of the zwitterionic structures in which the N<sub>ε</sub>H group and one of the N<sub>γ</sub>H<sub>2</sub> groups each donates one hydrogen bond to the amino acid backbone. The best agreement is obtained with structure **D1**, in which the metal ion is coordinated with the carboxylate group and the protonated side chain donates hydrogen bonds to both the N-terminal amino and the carboxylate groups. The experimentally observed bands are close in both frequency and relative intensity to calculated bands for free N<sub>γ</sub>H<sub>2</sub> symmetric stretch, bonded N<sub>γ</sub>H<sub>2</sub> asymmetric stretch, free N<sub>γ</sub>H<sub>2</sub> asymmetric stretch, water symmetric stretch, and water asymmetric stretch of structure **D1** (Table 2). Bands near 2950 and 3100 cm<sup>-1</sup> are well-explained by CH stretching modes and the bonded N<sub>γ</sub>H<sub>2</sub> symmetric stretch, respectively, although the relatively intensities of these bands are considerably less than expected from the calculations. Curiously, the bonded N<sub>ε</sub>H stretch, which is calculated to have the highest integrated oscillator strength, is absent in the IRMPD spectrum.

Although the high-frequency bands are very indicative of zwitterionic structures, the most intense band in each of the calculated spectra for these structures is below 3000 cm<sup>-1</sup>, and these are not observed experimentally (Table 2). The absence of analogous bands in the spectra of Arg•Na<sup>+</sup>, Arg•K<sup>+</sup>, and Arg•H<sup>+</sup> was primarily attributed to the limited frequency range of the previous experimental spectra which were only acquired

at frequencies greater than ~2600 cm<sup>-1</sup>. Frequencies are calculated using the harmonic oscillator approximation and may considerably overestimate the frequencies of these modes which are likely to have significant anharmonic character. The absence of analogous bands in the IRMPD spectrum of Arg•Na<sup>+</sup>(H<sub>2</sub>O), which exhibited no measurable photodissociation from 2000–2700 cm<sup>-1</sup>, somewhat weakens this possibility. However, recent experiments by Johnson and co-workers reveal that the stretching mode of shared protons can occur considerably to the red of this range; this band for the protonated homodimer of diethyl ether was observed at 843 cm<sup>-1</sup>.<sup>57</sup> Alternatively, the photodissociation efficiency for these modes under the conditions of experiment may be exceedingly low. This could be attributable to lower photon energies, limited multiple photon absorption due to reduced laser photon fluxes at these frequencies, or low-absorbance cross sections at a given frequency due to band broadening, and other factors.

Hydrogen stretch bands originating from strongly hydrogen-bonded groups have been conspicuously absent in the IR action spectra of other hydrated ions. For example, the photodissociation spectrum of H<sup>+</sup>(H<sub>2</sub>O)<sub>21</sub> does not exhibit photodissociation between 2000–3000 cm<sup>-1</sup>, expected for Eigen-like structures of this ion, which was attributed to inefficient photodissociation at lower photon energies, anharmonicity, or the presence of Zundel-like structures that are disfavored by theory.<sup>58</sup> Recent ab initio molecular dynamics simulations suggest that these bands for H<sup>+</sup>(H<sub>2</sub>O)<sub>21</sub> are extremely broad due to finite temperature effects and that the lack of measurable photodissociation in the 2000–3000 cm<sup>-1</sup> may be attributable to these effects.<sup>59</sup>

The photodissociation exhibited between 3200 and 3350 cm<sup>-1</sup> may indicate the presence of a population of ions in which the water molecule has disrupted one of the metal ion/carboxylate group interactions (**D1\***). Calculations indicate that structure **D1\*** is slightly favored over **D1** for Arg•Na<sup>+</sup>(H<sub>2</sub>O) at 0 and 200 K, although structure **D1** is preferentially stabilized with increasing temperature (Table 1). In this structure, the water asymmetric stretch red-shifts to 3049 cm<sup>-1</sup>, and the bonded N<sub>γ</sub>H<sub>2</sub> symmetric stretch blue-shifts to 3198 cm<sup>-1</sup>. Both of these modes are expected to be broad, and it is difficult to assign relative populations of **D1** and **D1\*** from the IRMPD spectra. Additionally, the IRMPD spectrum of Arg•Na<sup>+</sup>(H<sub>2</sub>O) also shares some similarities with the spectra calculated for structures **G1** and **H1**, which are calculated to be 12 and 26 kJ/mol higher in free energy at 200 K than **D1**, respectively. Note that the

(57) Roscioli, J. R.; McCunn, L. R.; Johnson, M. A. *Science* **2007**, *316*, 249–254.

(58) Shin, J. W.; Hammer, N. I.; Diken, E. G.; Johnson, M. A.; Walters, R. S.; Jaeger, T. D.; Duncan, M. A.; Christie, R. A.; Jordan, K. D. *Science* **2004**, *304*, 1137–1140.

(59) Iyengar, S. S. *J. Chem. Phys.* **2007**, *126*, 216101.



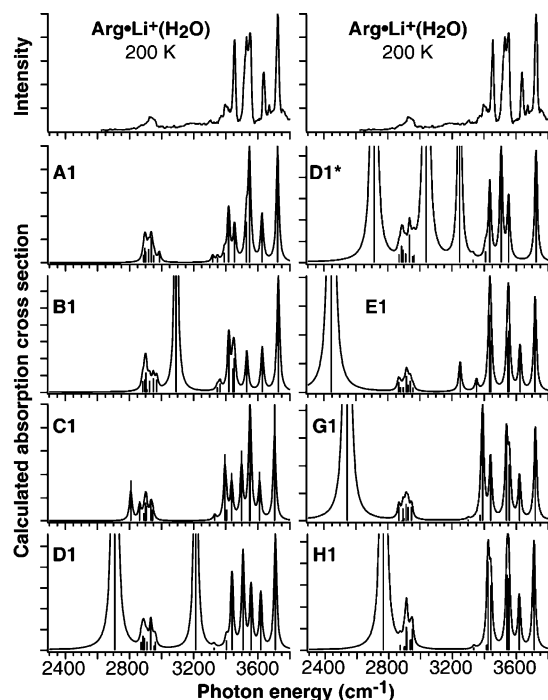


**Figure 5.** Photodissociation spectrum of  $\text{Arg}\bullet\text{Li}^+(\text{H}_2\text{O})$  and B3LYP/6-31++G\*\* calculated spectra for selected conformers of this ion. The intensities of the calculated spectra are scaled to the higher-frequency bands in the spectra. Un-normalized spectra and additional calculated spectra are shown in Supporting Information Figure 5–7.

populations of these structures are expected to be very small if the calculated relative energies are accurate and the precursor ions are well equilibrated with the surrounding copper jacket ( $T = 200$  K). In these structures, the  $\text{N}_\epsilon\text{H}$  group and one  $\text{N}_\eta\text{H}_2$  group donate one strong and one weak hydrogen bond to one oxygen atom of the carboxylate group, respectively. Because the guanidinium side chains in these structures donate hydrogen bonds somewhat similar to those for **D1**, the free NH stretches from for these groups are also somewhat similar. However, asymmetric stretch modes for the donor  $\text{N}_\eta\text{H}_2$  groups are calculated to occur at 3373 and 3311  $\text{cm}^{-1}$  for **G1** and **H1**, respectively, which should be observed experimentally as a resolved, albeit broad, band analogous to that observed for  $\text{Arg}\bullet\text{Li}^+(\text{H}_2\text{O})$ . Therefore, although the experimental and theoretical results are most consistent with **D1**, contributions from alternate zwitterionic structures in which the guanidinium side chain donates one strong and one weak hydrogen bond to the amino acid backbone cannot be completely ruled out.

**Structure of  $\text{Arg}\bullet\text{Li}^+(\text{H}_2\text{O})$ .** The IRMPD spectrum of  $\text{Arg}\bullet\text{Li}^+(\text{H}_2\text{O})$  resembles that of  $\text{Arg}\bullet\text{Na}^+(\text{H}_2\text{O})$ , suggesting that the structures for the two ions are similar and almost certainly zwitterionic. However, there are subtle differences between the two action spectra: the lower-frequency  $\text{N}_\eta\text{H}_2$  asymmetric stretch shifts from 3510  $\text{cm}^{-1}$  in  $\text{Arg}\bullet\text{Na}^+(\text{H}_2\text{O})$  to 3530  $\text{cm}^{-1}$  in  $\text{Arg}\bullet\text{Li}^+(\text{H}_2\text{O})$ , the broad band centered near 3100  $\text{cm}^{-1}$  in  $\text{Arg}\bullet\text{Na}^+(\text{H}_2\text{O})$  is absent in the spectrum obtained for the lithiated cluster, and there is significantly increased relative photodissociation at 3400  $\text{cm}^{-1}$  in the IRMPD spectrum of  $\text{Arg}\bullet\text{Li}^+(\text{H}_2\text{O})$ . Because the calculated spectra for structure **D1** for these ions are essentially indistinguishable (Figures 4 and 5), the subtle differences between the two IRMPD spectra suggest a different zwitterionic structure for  $\text{Arg}\bullet\text{Li}^+(\text{H}_2\text{O})$ .

The IRMPD spectrum of  $\text{Arg}\bullet\text{Li}^+(\text{H}_2\text{O})$  is similar to the calculated spectrum of structure **G1**. In this structure, the metal ion is coordinated with the N-terminal amino group and one oxygen atom of the carboxylate group, and the protonated side chain donates a hydrogen bond to the other oxygen atom of the carboxylate group. The experimentally observed bands are close in both frequency and relative intensity to those calculated bands for free  $\text{N}_\eta\text{H}_2$  symmetric stretch, bonded  $\text{N}_\eta\text{H}_2$  asymmetric stretch, free  $\text{N}_\eta\text{H}_2$  asymmetric stretch, water symmetric stretch, and water asymmetric stretch of structure **G1** (Table 2). The band centered near 3400  $\text{cm}^{-1}$  and assigned to the weakly bonded  $\text{N}_\eta\text{H}_2$  symmetric stretch (3389  $\text{cm}^{-1}$ ) is considerably broader than many of the other bands in the spectra. Due to the interactions between this  $\text{N}_\eta\text{H}_2$  group and the carboxylate group, it is likely that the frequency of this mode is especially sensitive to minor changes in side-chain conformation or excited torsions in the ion. The broad, albeit weak, photodissociation observed to the red of this band ( $\sim 3000$ – $3350$   $\text{cm}^{-1}$ ) may originate from structures of the **G1** structural motif, in which this  $\text{N}_\eta\text{H}_2$  group donates a stronger hydrogen bond to the carboxylate, or perhaps contributions from small populations of other zwitterionic structures.

The agreement between the experimental spectrum and the calculated absorbance spectra is poorer for  $\text{Arg}\bullet\text{Li}^+(\text{H}_2\text{O})$  than it is for either  $\text{ArgOMe}\bullet\text{Li}^+(\text{H}_2\text{O})$  or  $\text{Arg}\bullet\text{Na}^+(\text{H}_2\text{O})$ . This may be due to a number of reasons, including the possibility that the lowest-energy form of this ion was not identified or that the uncertainties in the calculated spectra for this ion are greater. The spectra may also be a composite of several structures, thus complicating the structural assignment of this ion. The strong similarities between the action spectra of  $\text{Arg}\bullet\text{Li}^+(\text{H}_2\text{O})$  and  $\text{Arg}\bullet\text{Na}^+(\text{H}_2\text{O})$  and the differences with those measured for  $\text{Arg}\bullet\text{Li}^+$  and  $\text{ArgOMe}\bullet\text{Li}^+(\text{H}_2\text{O})$  provide compelling evidence that  $\text{Arg}\bullet\text{Li}^+(\text{H}_2\text{O})$  adopts a zwitterionic structure. However, the lack of a unique match between the measured and calculated spectra for  $\text{Arg}\bullet\text{Li}^+(\text{H}_2\text{O})$  results in some ambiguity about which zwitterionic structure or structures are formed.

**Effect of Metal Ion Size on the Structure of Cationized Arginine.** Increasing metal ion size has been shown to preferentially stabilize the zwitterionic form of cationized arginine.<sup>38–40</sup> Lithiated Lys and  $\epsilon$ -N-Me-Lys are both nonzwitterionic and have no intramolecular hydrogen bonds, and the metal ion is solvated by the carbonyl oxygen, the N-terminal amino group, and side-chain amino groups.<sup>31</sup> The potassiated forms of these ions have different structures, containing only two interactions between the metal ion and the amino acid and at least one intramolecular hydrogen bond.<sup>31</sup> Interactions between a metal ion and a given amino acid should be the strongest for lithium of all the alkali metal ions, whereas the strengths of any hydrogen bonds should be roughly similar in complexes with all alkali metal ions. The zwitterionic structures of  $\text{Arg}\bullet\text{M}^+$  all contain at least one intramolecular hydrogen bond, whereas the lowest-energy nonzwitterionic forms contain no hydrogen bonds. On the basis of the reasons discussed above for cationized lysine, decreasing ligand binding energies with increasing metal ion size appear to be a dominant driving force in the formation of zwitterionic structures with increasing metal ion size.

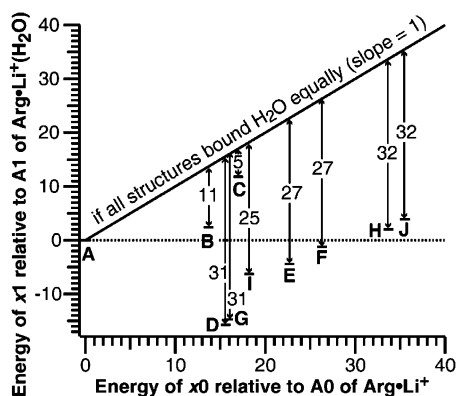


**Figure 6.** The B3LYP/6-31++G\*\* energies (in kJ/mol, including zero-point energies) of the  $x1$ ,  $x = A-J$ , structures of  $\text{Arg}\bullet\text{Li}^+(\text{H}_2\text{O})$  plotted versus those of the corresponding  $x0$  structures of  $\text{Arg}\bullet\text{Li}^+$ . These data for  $M = \text{Na}$  are presented in Supporting Information Figure 8.

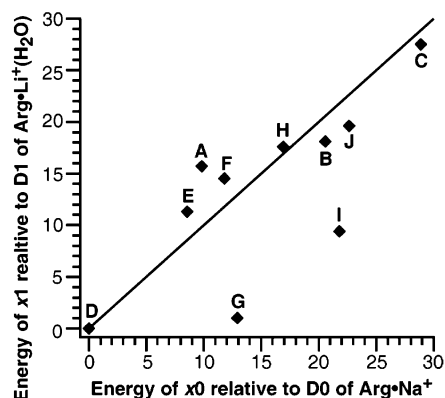


**Figure 7.** The B3LYP/6-31++G\*\* energies (in kJ/mol, including zero-point energies) of the  $x1$ ,  $x = A-J$ , structures of  $\text{Arg}\bullet\text{Li}^+(\text{H}_2\text{O})$  plotted versus those of the corresponding  $x0$  structures of  $\text{Arg}\bullet\text{Na}^+$ . The plotted line has a slope of unity.

**Effect of One Water Molecule on the Structure of Lithiated Arginine.** IRMPD spectra indicate that  $\text{Arg}\bullet\text{Li}^+$  is nonzwitterionic, whereas  $\text{Arg}\bullet\text{Li}^+(\text{H}_2\text{O})$  is zwitterionic. Comparing the experimental and computational results for these two ions reveals how solvation by just one water molecule drives the formation of the solution-phase, zwitterionic structure. If the first water binding energy to each structural family were the same, then the relative energies of  $x1$  would equal those of  $x0$ . Figure 6 shows that these values are not well correlated and the addition of one water molecule preferentially stabilizes the zwitterionic forms of lithiated arginine by 25–32 kJ/mol relative to the lowest-energy nonzwitterionic form.

Interestingly, the correlation between the relative energies of the  $\text{Arg}\bullet\text{Na}^+$  and  $\text{Arg}\bullet\text{Li}^+(\text{H}_2\text{O})$  conformers is much better (Figure 7), suggesting that solvating  $\text{Arg}\bullet\text{Li}^+$  with one water molecule has a similar effect to substituting Na for Li in  $\text{Arg}\bullet\text{M}^+$ . Solvating a metal ion decreases all subsequent ligand binding energies. For example, the first four water binding energies to  $\text{Li}^+$  are roughly 140, 110, 90, and 70 kJ/mol, respectively, whereas those values for Na are roughly 95, 80, 65, and 55 kJ/mol.<sup>60–62</sup> To a very crude approximation, the second, third, and fourth water binding energies to  $\text{Li}^+$  are close

to the first, second, and third water binding energies to  $\text{Na}^+$ . It is therefore reasonable to expect that some of the ligand binding properties of  $\text{Li}^+(\text{H}_2\text{O})$  may be similar to those of  $\text{Na}^+$ . This appears to be the case for structural families A–F, H, and J, wherein the relative energies of the structural motifs of  $\text{Arg}\bullet\text{Na}^+$  and  $\text{Arg}\bullet\text{Li}^+(\text{H}_2\text{O})$  are nearly directly related. In contrast, zwitterionic structures G and I of  $\text{Arg}\bullet\text{Li}^+(\text{H}_2\text{O})$  are especially stable relative to those structures of  $\text{Arg}\bullet\text{Na}^+$ . The metal ion in structures G and I is coordinated to the N-terminal amino group and an oxygen atom of the carboxylate group (NO coordinated), whereas it is coordinated to both oxygen atoms of the carboxylate group (OO coordinated) in the remaining zwitterionic structures. This shows a strong ion-specific preference for one binding site (NO coordination for lithium) versus another (OO coordination for sodium) in zwitterionic arginine.

Similar specific-ion effects have been observed for alkali metal-cationized glycine. The metal ion in the lowest-energy structure of  $\text{Gly}\bullet\text{Li}^+$  is NO-coordinated and nonzwitterionic.<sup>63</sup> The OO-coordinated, nonzwitterionic structure of  $\text{Gly}\bullet\text{Li}^+$  is 45 kJ/mol higher in energy, but increasing metal ion size preferentially stabilizes this structure, and it is lowest in energy for  $\text{Gly}\bullet\text{M}^+$ ,  $M = \text{K}, \text{Rb}, \text{and Cs}$ .<sup>63</sup> The metal ion in the NO-coordinated structures of  $\text{Gly}\bullet\text{M}^+$  and  $\text{Arg}\bullet\text{M}^+$  completes a five-member ring; this ring structure becomes distorted and less stable relative to the OO-coordinated structure with increasing metal ion size for  $\text{Gly}\bullet\text{M}^+$ .<sup>63</sup> It appears that similar size constraints in the N-terminal amino group/oxygen atom binding pocket of zwitterionic arginine drive the formation of an NO-coordinated structure for  $\text{Arg}\bullet\text{Li}^+(\text{H}_2\text{O})$  and an OO-coordinated structure for  $\text{Arg}\bullet\text{Na}^+(\text{H}_2\text{O})$ .

**Effects of Theoretical Approach.** In order to evaluate the effectiveness of the density functional (B3LYP) and basis set (6-31++G\*\*), which have been used previously to describe a variety of similar ions,<sup>16,18,22,24,26,31,38</sup> additional calculations were performed on structures A1, D1, D1\*, and G1 of  $\text{Arg}\bullet\text{Li}^+(\text{H}_2\text{O})$ , and these results are summarized in Table 3. Removing the diffuse functions (6-31G\*\* and 6-31+G\*\*) from the extended Pople basis set used in the majority of the calculations (6-31++G\*\*) has a very minor effect on the relative energies of these structures (1–4 kJ/mol). Relative B3LYP/6-311++G-(2d,2p)//6-31++G(\*\*) energies are also quite similar, suggesting that the relative B3LYP energies are reasonably well converged even with the modest 6-31G\*\* basis set. The Dunning correlation-consistent cc-pVDZ basis set, which includes polarizable functions, but no diffuse functions, preferentially favors nonzwitterionic structure A1 by ~10 kJ/mol relative to the zwitterionic structures. However, much of this difference is mitigated when the triple- $\zeta$  contraction of this basis set is used (B3LYP/cc-pVTZ//cc-pVDZ); the relative energies from these calculations are almost identical to those obtained with triple- $\zeta$  quality Pople basis set (B3LYP/6-311++G(2d,2p)//6-31++G(\*\*)).

Using more accurate treatments of electron correlation has a larger effect on the relative energies of these structures. For most of these calculations, diffuse basis set functions were not included, which has a minor effect on the relative B3LYP energies. The “resolution-of-the-identity” (RI) approximation of Møller–Plesset second-order perturbation theory (MP2) has been shown to be considerably more efficient than standard

(60) Rodgers, M. T.; Armentrout, P. B. *J. Phys. Chem. A* **1997**, *101*, 1238–1249.

(61) Dzidic, I.; Kobar, P. *J. Phys. Chem.* **1970**, *74*, 1466–1474.

(62) Dalleska, N. F.; Tjelta, B. L.; Armentrout, P. B. *J. Phys. Chem.* **1994**, *98*, 4191–4195.

(63) Hoyau, S.; Ohanessian, G. *Chem.—Eur. J.* **1998**, *4*, 1561–1569.



MP2, yet only introduces small additional errors.<sup>54,64,65</sup> Compared to B3LYP/cc-pVDZ and relative to structure **D1**, structure **A1** is preferentially stabilized by 17 kJ/mol at the RI-MP2/cc-pVDZ level of theory, whereas structures **D1\*** and **G1** are destabilized by 6 and 9 kJ/mol, respectively. Interestingly, RIMP2/cc-pVDZ energy minimization of the B3LYP/6-31++G\*\* geometries stabilizes each of the structures by 6–7 kJ/mol, so that the relative RIMP2/cc-pVDZ and RIMP2/cc-pVDZ/B3LYP/6-31++G\*\* energies of the structures are essentially identical. These values are also very similar to those obtained using MP2/cc-pVDZ/RIMP2/cc-pVDZ, indicating the RI approximation does not introduce significant errors compared to MP2 for these systems. Single-point calculations with a more complete basis set (RIMP2/cc-pVTZ//cc-pVDZ) preferentially favor the zwitterionic structures by ~10 kJ/mol relative to RIMP2/cc-pVDZ.

Interestingly, the B3LYP results appear to be in better agreement with the experimental results than those from the MP2-based methods. The spectrum of  $\text{Arg}\cdot\text{Li}^+(\text{H}_2\text{O})$  is clearly indicative of a zwitterionic structure, yet most of the MP2-based results indicate that the nonzwitterionic form (**A1**) of this ion is lowest in energy. MP2/6-311++G\*\*/B3LYP/6-31++G\*\* predicts this correctly, although the lowest-energy zwitterionic and nonzwitterionic forms are very close in energy. The RIMP2/cc-pVTZ//cc-pVDZ results suggest that convergence with respect to basis set size has not been achieved with the double- $\zeta$  quality basis set and that the use of even larger basis sets may further favor the zwitterionic forms of  $\text{Arg}\cdot\text{Li}^+(\text{H}_2\text{O})$ . The spectrum of  $\text{Arg}\cdot\text{Li}^+(\text{H}_2\text{O})$  is arguably the most consistent with structure **G1**, yet this structure is calculated to be at least 9 kJ/mol higher in energy than **D1** for all of the MP2-based methods (+20 kJ/mol for MP2/6-311++G\*\*/B3LYP/6-31++G\*\*), whereas those structures are essentially isoenergetic in the B3LYP calculations utilizing larger basis sets. This discrepancy is greatest for MP2/6-311++G\*\*/B3LYP/6-31++G\*\*, for which structure **G1** is 20 kJ/mol higher in energy than **D1**. These results suggest that the B3LYP calculations provide reasonable predictive insights into these systems, even with modest basis sets, whereas very large basis sets are required for the MP2-based methods to converge reasonably with experiment. It is difficult to assess the uncertainties in these calculations, but these results indicate that the uncertainty for values reported elsewhere in the manuscript is almost certainly greater than 5 kJ/mol.

**BIRD of  $\text{Arg}\cdot\text{M}^+(\text{H}_2\text{O})_{1-3}$ : Insights into the Structures of Larger Clusters.** Blackbody infrared radiative dissociation (BIRD) kinetics for the loss of one water molecule from  $\text{Arg}\cdot\text{M}^+(\text{H}_2\text{O})_n$ , for  $\text{M} = \text{Li}$  and  $\text{Na}$ , and  $n = 1-3$ , were measured at 240 K, and are shown in Figure 8 (rate constants are reported in Table 4). Pressures less than  $10^{-8}$  Torr were achieved prior to ion isolation, indicating that these data were acquired in the zero-pressure limit.<sup>55,66–68</sup> In this limit, measured BIRD rates depend on the radiative absorption and emission rates, the threshold dissociation energy for the loss of the water molecule, and the transition-state entropy, although this latter

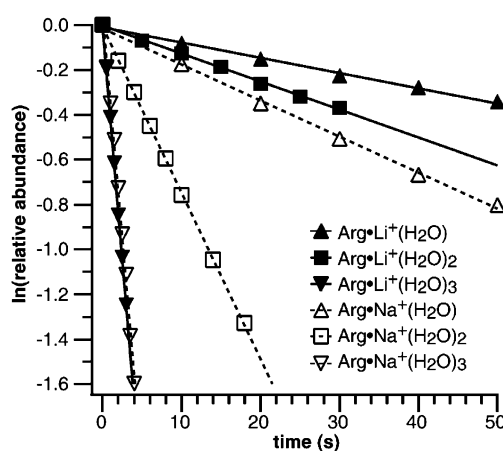


**Figure 8.** Blackbody infrared radiative dissociation kinetics at 240 K for the loss of one water molecule from  $\text{Arg}\cdot\text{Li}^+(\text{H}_2\text{O})_{1-3}$  and  $\text{Arg}\cdot\text{Na}^+(\text{H}_2\text{O})_{1-3}$ . Precursor identities are labeled on the figure.

**Table 4.** Blackbody Infrared Radiative Dissociation Rate Constants at 240 K for the Loss of One Water Molecule from  $\text{Arg}\cdot\text{M}^+(\text{H}_2\text{O})_{1-3}$ ,  $\text{M} = \text{Li}$  and  $\text{Na}$

precursor identity	rate ( $\text{s}^{-1}$ ), $\text{M} = \text{Li}$	rate ( $\text{s}^{-1}$ ), $\text{M} = \text{Na}$
$\text{Arg}\cdot\text{M}^+(\text{H}_2\text{O})$	$0.0068 \pm 0.0002$	$0.0161 \pm 0.0004$
$\text{Arg}\cdot\text{M}^+(\text{H}_2\text{O})_2$	$0.0124 \pm 0.0002$	$0.0741 \pm 0.0004$
$\text{Arg}\cdot\text{M}^+(\text{H}_2\text{O})_3$	$0.419 \pm 0.004$	$0.40 \pm 0.01$

factor likely has only a minimal effect for these relatively small ions under these conditions.<sup>67,68</sup> Because the lithiated and sodiated ions of a given  $n$  have identical degrees of freedom and should have similar blackbody absorption cross sections, the differences in dissociation rates should primarily be due to differences in the dissociation energies for the loss of a water molecule.

The BIRD rates for the lithiated and sodiated ions thus provide some insights into the structures of these ions. For  $n = 1$  and 2, the rate constants for the sodiated ions are significantly greater than those of the corresponding lithiated ions. This is consistent with both water molecules interacting with the metal ion, because water molecule binding energies to sodium ions are smaller than those to lithium ions<sup>60–62</sup> or with different water coordination sites in the two ions. In contrast, the BIRD rates for the ions with  $n = 3$  are almost indistinguishable. This suggests that the third water molecule does not play a significant role in solvating the metal ion for  $\text{Arg}\cdot\text{Li}^+(\text{H}_2\text{O})_3$  and  $\text{Arg}\cdot\text{Na}^+(\text{H}_2\text{O})_3$  and may be bound to the guanidinium side chain.

## Conclusions

Both experiment and theory indicate that the addition of just a single water molecule has a profound effect on the structure of lithiated arginine. Hydration of the lithium ion changes its binding properties and preferentially stabilizes the zwitterionic forms of this cluster by 25–32 kJ/mol relative to the lowest-energy nonzwitterionic structure. Zwitterionic structures of  $\text{Arg}\cdot\text{Li}^+(\text{H}_2\text{O})$  are the lowest-energy forms and are observed experimentally. These results show that solvation of a cluster by even a single water molecule can convert the most favorable gas-phase structure of arginine into the zwitterionic form. This suggests that detailed information about the effects of explicit solvation on biomolecular structure can be obtained by studying hydrated ions in the gas phase. Such studies may provide particularly relevant insights into the structures of biomolecules

(64) Weigend, F.; Haser, M.; Patzelt, H.; Ahlrichs, R. *Chem. Phys. Lett.* **1998**, *294*, 143–152.

(65) Distasio, R. A.; Steele, R. P.; Rhee, Y. M.; Shao, Y. H.; Head-Gordon, M. *J. Comput. Chem.* **2007**, *28*, 839–856.

(66) Dunbar, R. C.; McMahon, T. B. *Science* **1998**, *279*, 194–197.

(67) Price, W. D.; Williams, E. R. *J. Phys. Chem. A* **1997**, *101*, 8844–8852.

(68) Price, W. D.; Schnier, P. D.; Williams, E. R. *J. Phys. Chem. B* **1997**, *101*, 664–673.

in low-dielectric environments, such as the interiors of proteins or cell membranes.

The data are most consistent with the singly hydrated lithiated and sodiated ions forming different zwitterionic structures. The metal ion in  $\text{Arg}\bullet\text{Li}^+(\text{H}_2\text{O})$  is coordinated with the N-terminal amino group, an oxygen atom of the carboxylate group, and the oxygen atom of the water molecule (NO coordinated), whereas that in  $\text{Arg}\bullet\text{Na}^+(\text{H}_2\text{O})$  is coordinated with both oxygen atoms of the carboxylate group and the oxygen atom of the water molecule (OO coordinated). Differences in metal ion size strongly affect the relative propensity for these ions to form NO- and OO-coordinated structures and result in different zwitterionic structures for the lithiated and sodiated ions. These results show that gas-phase clusters are excellent systems for studying specific-ion effects, such as Hofmeister series effects,<sup>69</sup>

(69) Kunz, W.; Lo Nostro, P.; Ninham, B. W. *Curr. Opin. Colloid Interface Sci.* **2004**, 9, 1–18.

since the effects of counterions and solvation can be explicitly controlled by varying the composition of the cluster.

**Acknowledgment.** Generous financial support was provided by the National Science Foundation (Grants CHE-0718790 (E.R.W.) and CHE-0404571 (R.J.S.)). We thank Professor Alan G. Marshall and Dr. Gregory T. Blakney (National High Magnetic Field Laboratory) for the loan of, assistance with, and support for a modular FT/ICR data acquisition system (MIDAS) used in these studies. M.F.B. thanks Prof. Martin P. Head-Gordon for useful discussions.

**Supporting Information Available:** Cartesian coordinates for all structures, Supporting Information Figures 1–8, and full citation for reference 54. This material is available free of charge via the Internet at <http://pubs.acs.org>.

JA073796B